

University of Nebraska - Lincoln

DigitalCommons@University of Nebraska - Lincoln

Roger Kirby Publications

Research Papers in Physics and Astronomy

November 1975

Effect of uniaxial stress on the unstable A_1 (TO) phonon in ferroelectric gadolinium molybdate

B.N. Ganguly

University of Nebraska - Lincoln

Frank G. Ullman

University of Nebraska - Lincoln

Roger D. Kirby

University of Nebraska-Lincoln, rkirby1@unl.edu

J.R. Hardy

University of Nebraska - Lincoln

Follow this and additional works at: https://digitalcommons.unl.edu/physics_kirby



Part of the [Physics Commons](#)

Ganguly, B.N.; Ullman, Frank G.; Kirby, Roger D.; and Hardy, J.R., "Effect of uniaxial stress on the unstable A_1 (TO) phonon in ferroelectric gadolinium molybdate" (1975). *Roger Kirby Publications*. 39.

https://digitalcommons.unl.edu/physics_kirby/39

This Article is brought to you for free and open access by the Research Papers in Physics and Astronomy at DigitalCommons@University of Nebraska - Lincoln. It has been accepted for inclusion in Roger Kirby Publications by an authorized administrator of DigitalCommons@University of Nebraska - Lincoln.

Effect of uniaxial stress on the unstable $A_1(\text{TO})$ phonon in ferroelectric gadolinium molybdate*

B. N. Ganguly,[†] Frank G. Ullman, R. D. Kirby, and J. R. Hardy

Department of Physics, University of Nebraska, Lincoln, Nebraska 68508

(Received 6 January 1975)

The effect of uniaxial stress along [100] on the unstable $A_1(\text{TO})$ phonon, 47 cm^{-1} at room temperature, in ferroelectric ($<159^\circ\text{C}$) gadolinium molybdate has been studied by Raman scattering at 138, 141, 146, and 155°C . An increase in peak frequency and narrowing of the line shape is observed with increasing stress. The data are analyzed by fitting to a Lorentzian line shape. The force-constant parameter is insensitive to both stress and temperature, whereas the damping constant decreases nonlinearly with stress, approaching an asymptotic value at high stress.

I. INTRODUCTION

Gadolinium molybdate (GMO) and its isomorphs were the first of a class of new materials, now termed "improper ferroelectrics,"¹ for which the dynamics of the ferroelectric phase transition was studied.² Those neutron scattering studies established that the ionic displacements from the paraelectric phase to form the ferroelectric phase could be correlated with the eigenvectors of two degenerate M -point phonons of the paraelectric phase. The frequency of these two phonons was found to decrease with temperature in a manner consistent with Curie-Weiss dielectric behavior, and to fall to zero discontinuously at the 159°C first-order-transition temperature T_0 , at which the crystallographic cell doubles and rotates 45° about the unique axis. The behavior of the A_1 phonons in the ferroelectric phase that are derived from these soft zone-boundary phonons has not yet been established. Fleury³ observed, at room temperature and above, an $A_1(\text{TO})$ mode in Raman scattering from GMO, with a room-temperature peak at 47 cm^{-1} , which shifted to lower frequencies on heating and which broadened until it merged with the background close to T_0 . No corresponding modes were found above T_0 . A Lorentzian analysis showed that the force-constant parameter ω_0 decreased only slightly from room temperature up to T_0 , but the damping constant increased superlinearly. A similar temperature dependence above room temperature was observed in infrared absorption⁴; at lower temperatures the infrared line resolved into a doublet.⁴ In Raman scattering studies in this laboratory, Fleury's data were reproduced and the splitting at lower temperature, observed in ir absorption, could also be seen.⁵

The work described here was stimulated by a report⁶ that the small anomaly in the unclamped dielectric constant of GMO at T_0 (Ref. 7) shifted to higher temperature by 29.5°C per kilobar of hydrostatic pressure. If the unstable 47-cm^{-1}

$A_1(\text{TO})$ mode is indeed associated with the ferroelectric transition, a similar change with pressure should be observable in Raman scattering. For convenience, we chose to use uniaxial stress rather than hydrostatic pressure; the description of our observations of the changes in the 47-cm^{-1} mode with increasing uniaxial stress is the subject of this paper.

II. EXPERIMENTAL DETAILS

Raman spectra were measured with a Spex, model 1401, double monochromator with spectral resolution better than 2 cm^{-1} . The excitation source was a Coherent Radiation Laboratory, model 52, argon-ion laser. The signal was detected with a thermoelectrically cooled EMI 9502BA photomultiplier tube along with conventional photon-counting electronics. A broad fluorescent background was present with 4880-\AA excitation; hence all the spectra were taken with 5145-\AA excitation. The laser power was limited to less than 400 mW to avoid thermal damage to the sample. The samples were cut from a boule purchased from the Isomet Corporation. To study the effect of up to a few kilobars of pressure on the phase transition, a uniaxial stress cell that could be mounted on the Raman spectrometer was designed. Only $A_1(\text{TO})$ phonons, using the scattering geometry $x(zz)y$, were studied with the stress applied along [100], i.e., parallel to the incident beam. Since the samples could not be kept single domain at zero stress, the x and y directions are not unique in that case, and can be interchanged. This, however, mixes only the B_1 and B_2 Raman spectra and thus had no bearing on these measurements.

With this stress direction, the plunger and support base have to be transparent. The support base and plunger each consisted of a 1-in. diameter 0.5 in. thick optically flat fused-silica window, as shown in the schematic diagram of the stress cell in Fig. 1. The sample was thermally anchored to

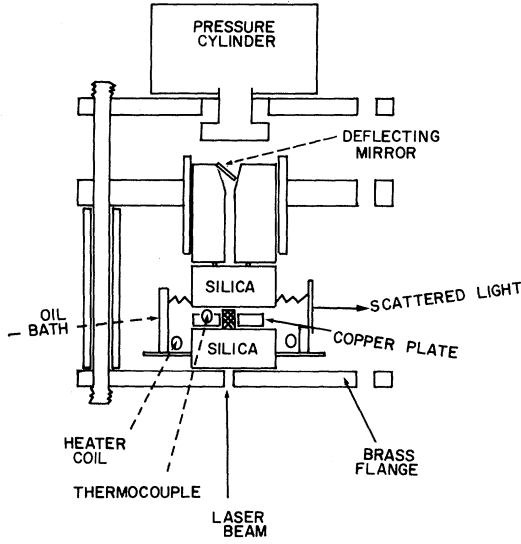


FIG. 1. Schematic diagram of uniaxial stress cell.

a copper plate and was immersed in Edwards 705 silicone oil along with a heater coil wrapped in teflon tape. The temperature of the oil bath was controlled by varying the heater-coil current manually. The sample temperature was measured with a copper-constant thermocouple. The temperature was held within $\pm 0.5^\circ\text{C}$ of the desired temperature during each spectral scan. The temperature resolution was $\pm 0.15^\circ\text{C}$.

III. EXPERIMENTAL RESULTS

The right-angle-scattered $A_1(\text{TO})$ Raman spectrum in the $0\text{--}65\text{ cm}^{-1}$ range was measured for applied stresses ranging from 0 to about 3 kbar. The spectra were taken in steps of approximately 0.25 kbar at each of four temperatures: 138, 141, 146, and 155°C . The overall effect of the applied stress was to increase the peak frequency ω_p and to decrease the linewidth. The change in peak frequency ω_p with stress is shown in Fig. 2. The observed spectra were analyzed by assuming a Lorentzian line shape. The Raman intensity of a Stokes line, in this case,⁸ is

$$I(\omega) = A \left[(e^{\hbar\omega/kT} - 1)^{-1} + 1 \right] \times \left\{ \omega_0^3 \Gamma \omega \chi(0) / [(\omega_0^2 - \omega^2)^2 + 4\Gamma^2 \omega_0^2 \omega^2] \right\}, \quad (1)$$

in which the damping constant Γ is assumed to be frequency independent, $\chi(0)$ is the static electric susceptibility, and A is a proportionality constant.

Normalizing to the peak intensity gives

$$\frac{\omega I(\omega_p)(1 - e^{-\hbar\omega_p/kT})}{\omega_p I(\omega)(1 - e^{-\hbar\omega/kT})} = \left[\frac{\omega_0^4 - 2\omega_0^2 \omega^2 (1 - 2\Gamma^2) + \omega^4}{(\omega_0^2 - \omega^2)^2 + 4\Gamma^2 \omega_0^2 \omega^2} \right]. \quad (2)$$

The right-hand side of Eq. (2) can be written in the form $A_1 + A_2 x + A_3 x^2$, where

$$\begin{aligned} A_1 &= \omega_0^4 / [(\omega_0^2 - \omega_p^2)^2 + 4\Gamma^2 \omega_0^2 \omega_p^2], \\ A_2 &= -2\omega_0^2 (1 - 2\Gamma^2) / [(\omega_0^2 - \omega_p^2)^2 + 4\Gamma^2 \omega_0^2 \omega_p^2], \\ A_3 &= [(\omega_0^2 - \omega_p^2)^2 + 4\Gamma^2 \omega_0^2 \omega_p^2]^{-1}, \\ x &= \omega^2. \end{aligned}$$

The force-constant parameter ω_0 and the damping constant Γ could be obtained from a three-parameter (ω_0 , Γ , and ω_p) least-squares fit if ω_0 and Γ were independent. However, they are not when ω_p is used to fit the data to the Lorentzian. The condition that the line intensity have a maximum, $dI(\omega)/d\omega|_{\omega=\omega_{\text{peak}}} = 0$, gives the expression relating ω_0 and Γ as

$$\begin{aligned} \omega_0 &= \frac{\omega_p}{[1 - e^{-\hbar\omega/kT} (1 + \hbar\omega_p/kT)]^{1/2}} \\ &\times \left\{ (1 - 2\Gamma^2) [e^{-\hbar\omega_p/kT} (1 - \hbar\omega_p/kT) - 1] \right. \\ &+ \left. \left\{ (1 - 2\Gamma^2)^2 [e^{-\hbar\omega_p/kT} (1 - \hbar\omega_p/kT) - 1]^2 \right. \right. \\ &\left. \left. - [1 - e^{\hbar\omega_p/kT} (1 - \hbar\omega_p/kT)] \right\} \right. \\ &\left. \times [e^{-\hbar\omega_p/kT} (3 - \hbar\omega_p/kT) - 3] \right\}^{1/2}. \quad (3) \end{aligned}$$

If the $e^{\pm\hbar\omega/kT}$ terms are expanded and only the first power terms are retained, Eq. (3) reduces to the familiar form⁸

$$\omega_p = \omega_0 (1 - 2\Gamma^2)^{1/2}. \quad (4)$$

Thus, only two independent parameters are available for fitting the data to Eq. (2) to determine ω_0 and Γ .

It is essential in fitting these data that as precise

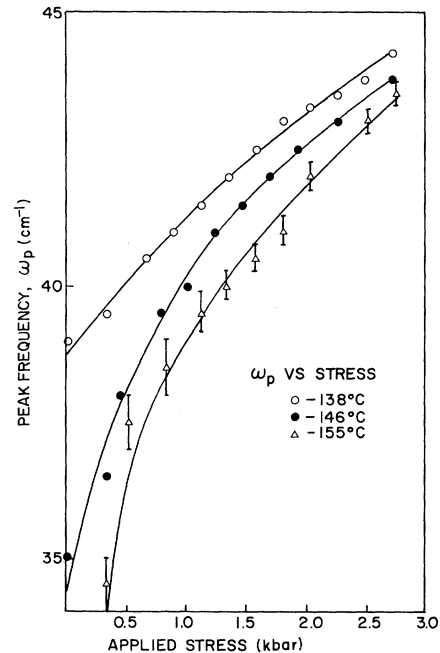


FIG. 2. Change in peak frequency with stress.

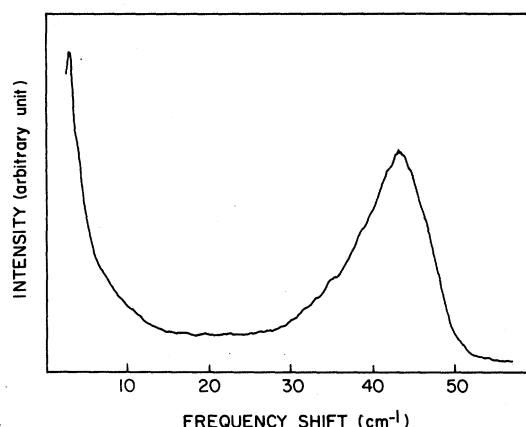


FIG. 3. Raman spectrum of the unstable mode at 128°C and 2.8 kbar.

as possible a correction be made for the superposed background, particularly for those spectra whose low-frequency portions merge with the background. A direct measurement of the background is not possible. In this work, the background correction was based on the assumption that the background was temperature independent over the range of these measurements, and thus if it could be computed for one specific case it could be used for all others. A spectrum for 128°C and 2.8 kbar, shown in Fig. 3, was selected as most favorable

since the linewidth was narrow enough to determine ω_p without a background correction. For such a narrow line, $\omega_0 \sim \Delta/\Gamma$, where Δ is the half-width at half-maximum. Substituting this expression for ω_0 in Eq. (4) results in

$$\Gamma = [2 + (\omega_p/\Delta)^2]^{-1/2}. \quad (5)$$

Using Eq. (5) and the measured values of ω_p and Δ , a value of Γ was computed and substituted into Eq. (4) to obtain ω_0 . The Lorentzian line for these values of Γ and ω_0 was then calculated. Initially, a reasonable estimate of the background spectrum could be made visually. Starting with that estimate, the final correction was determined by repeated trials to obtain the best fit between the measured spectrum, corrected for background, and the calculated Lorentzian line.

In Table I, the values of ω_0 , Γ , and ω_p are listed for all temperatures and applied stress. The stress dependences of Γ and of ω_0 are shown in Fig. 4 and 5, respectively. As can be seen, the major effect of the stress is on the damping, in agreement with Fleury's observations of the temperature dependence.³

Typical calculated and measured spectra at 146°C are shown in Fig. 6. The agreement between the calculated and measured spectra is reasonably good, although there are small but consistent deviations between the low- and high-frequency tails.

TABLE I. Calculated values of peak frequency ω_p , force-constant parameter ω_0 , and the damping constant Γ for the stresses and temperatures studied.

P (kbar)	ω_p (cm^{-1})	Γ	ω_0 (cm^{-1})	P (kbar)	ω_p (cm^{-1})	Γ	ω_0 (cm^{-1})
138°C				141°C			
0	39.0	0.2996	42.88	0.34	38.0	0.320	42.42
0.34	39.5	0.2836	42.94	0.58	39.0	0.3027	42.97
0.68	40.5	0.260	43.43	0.79	40.0	0.2734	43.23
0.9	41.0	0.2374	43.45	1.01	41.0	0.2464	43.63
1.14	41.5	0.2216	43.61	1.24	41.25	0.2348	43.63
1.36	42.0	0.1913	43.56	1.45	41.5	0.2127	43.43
1.58	42.5	0.1838	43.95	1.8	42.5	0.180	43.89
1.8	43.0	0.1702	44.25	2.03	43.0	0.170	44.25
2.03	43.25	0.1642	44.41	2.26	43.5	0.153	44.51
2.26	43.5	0.1479	44.44	2.76	44.5	0.133	45.27
2.71	44.0	0.1394	44.89				
146°C				155°C			
0	35.0	0.4479	44.05	0.34	34.5	0.446	43.95
0.34	36.5	0.394	43.59	0.56	37.5	0.388	44.5
0.58	38.0	0.354	43.63	0.86	38.75	0.335	43.77
0.79	39.5	0.315	43.64	1.14	39.5	0.300	43.45
1.01	40.0	0.286	43.3	1.32	40.0	0.2797	43.60
1.25	41.25	0.2485	43.94	1.58	40.5	0.248	43.13
1.46	41.5	0.2325	43.84	1.8	41.0	0.238	43.45
1.68	42.0	0.2135	43.97	2.03	42.0	0.220	44.12
1.92	42.5	0.1997	44.23	2.5	43.0	0.18	44.41
2.26	43.0	0.186	44.5	2.72	43.5	0.1736	44.81
2.71	43.75	0.1563	44.81				

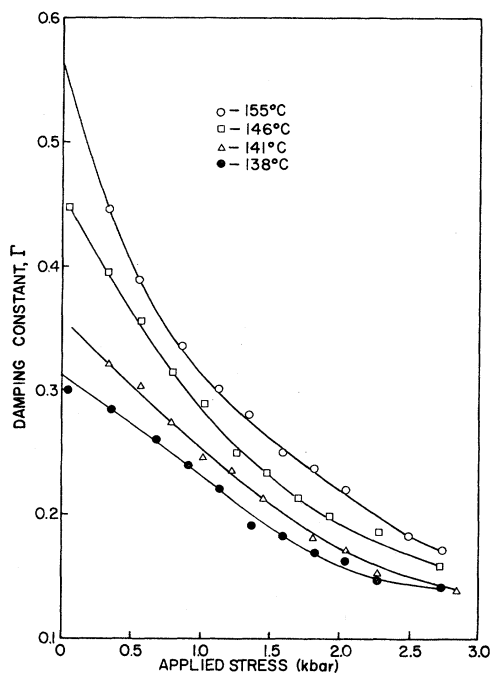


FIG. 4. Stress dependence of the damping constant Γ .

The calculated line shapes deviate systematically from the measured line shapes. In the lower-fre-

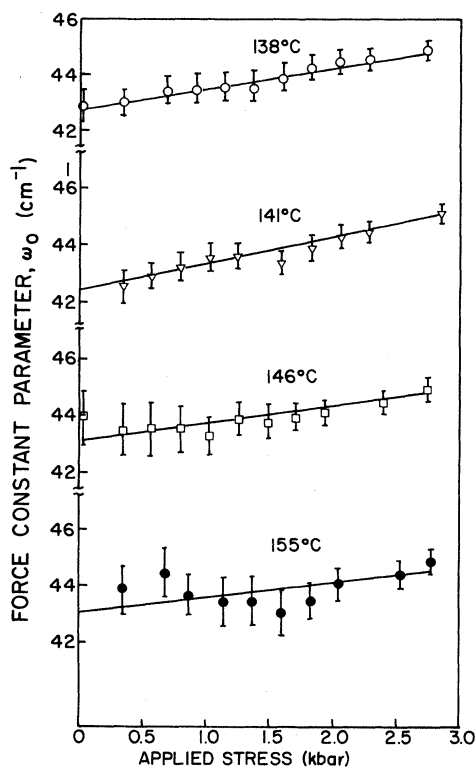


FIG. 5. Stress dependence of the force-constant parameter ω_0 .

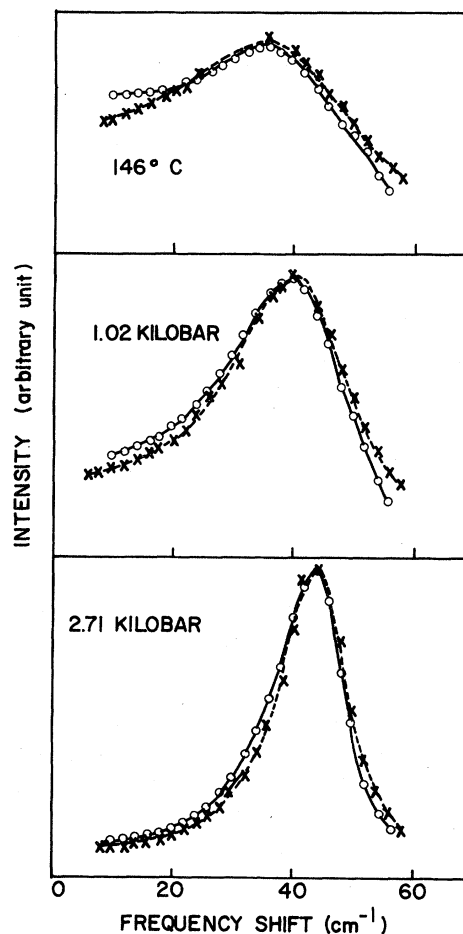


FIG. 6. Comparison of calculated and measured spectra at 146°C and 0-, 1.02-, and 2.71-kbar stress.

quency portion, the frequency of the maximum difference between the observed and calculated intensities shifts higher as the applied stress is increased, for all the spectra. (Some of this discrepancy may be due to this mode's actually consisting of two lines that are resolved below 200 °K.)

IV. DISCUSSION AND CONCLUSION

The two central features that emerge from the results of this study are the diverging nonlinear dependence of the damping on the applied stress and the absence of observable softening of the force constant parameter. Therefore the anomalous damping mechanisms that have been established for other materials for which a true soft mode is required, such as⁹ BaTiO₃ and¹⁰ potassium dihydrogen phosphate (KDP), cannot be operative in GMO. It would appear that the anomalies in the damping³ and the elastic constants¹¹ are not directly connected and must have their origin in some other yet undetermined loss mechanism.

*Research sponsored by the Air Force Office of Scientific Research, Office of Aerospace Research, USAF, under Grant No. AFOSR 70-1926.

†This work is based on a part of a dissertation submitted by B. N. Ganguly in partial fulfillment of the requirements for the Ph.D. degree.

‡Present address: Department of Chemistry, University of California, Los Angeles, California 90024.

¹V. Dvorak, Phys. Status Solidi B 45, 147 (1971).

²J. D. Axe, B. Dorner, and G. Shirane, Phys. Rev. Lett. 26, 519 (1971); B. Dorner, J. D. Axe, and G. Shirane, Phys. Rev. B 6, 1950 (1972).

³P. A. Fleury, Solid State Commun. 8, 601 (1970).

⁴J. Petzelt, Solid State Commun. 9, 1485 (1971).

⁵B. N. Ganguly, Ph.D. dissertation (unpublished).

⁶A. M. Shirokov, V. P. Mylov, A. I. Baranov, and T. M. Prokhortseva, Fiz. Tverd. Tela 13, 3108 (1971) [Sov. Phys.-Solid State 13, 2610 (1972)].

⁷L. E. Cross, A. Fouskova, and S. E. Cummins, Phys. Rev. Lett. 21, 812 (1968).

⁸M. DiDomenico, Jr., S. H. Wemple, and S. P. S. Porto, Phys. Rev. 174, 522 (1968).

⁹P. A. Fleury and P. D. Lazay, Phys. Rev. Lett. 26, 1331 (1971).

¹⁰E. M. Brody and H. Z. Cummins, Phys. Rev. Lett. 21, 1263 (1968).

¹¹U. F. Hochli, Phys. Rev. B 6, 1816 (1972).